Madany *et al. Egypt J Radiol Nucl Med* (2023) 54:50
https://doi.org/10.1186/s43055-023-00975-5

Egyptian Journal of Radiology and Nuclear Medicine

RESEARCH

Open Access

Magnetic resonance imaging in the workup of patients with perianal fistulas

Asmaa Hagagy Madany[1*], Amr Farouk Murad[2], Mansour Mohammed Kabbash[3] and Hala Maher Ahmed[1]

Abstract

Background Perianal sepsis and fistulas are common lesions. Fistula-in-ano is a tedious problem because of high recurrence rates and severe unexpected complications postoperatively. Many imaging modalities are used to evaluate this area. Magnetic resonance imaging (MRI) has been considered the gold standard procedure for perianal fistula assessment, i.e., it provides the surgeon with an accurate roadmap to select the best surgical approach, determines the extent of sphincter division, and estimates the risk of postoperative incontinence. We carried out a prospective diagnostic accuracy study involving 50 patients (mean age, 42.44 years) with perianal fistulas who underwent pelvic MRI with a 1.5 Tesla scanner using multiple sequences, including diffusion and post-contrast series that were either local or systemic. This study aimed to evaluate the diagnostic validity of pelvic MRI/MR fistulogram in perianal fistula assessment, identify perianal fistula-associated findings by MRI, and optimize the MRI technique with maximum technical safety.

Results Intersphincteric fistulas were the most common type of perianal fistula observed based on Parks' classification. Intersphincteric, trans-sphincteric, extrasphincteric, and suprasphincteric fistulas were found in 30 (60%), 12 (24%), 4 (8%), and 4 (8%) patients, respectively. According to St. James' classification, 21 (42%), 9 (18%), 8 (16%), 4 (8%), and 8 (16%) patients had perianal fistula grades I, II, III, IV, and V, respectively. The combination of variable MR sequences and MR fistulogram increased the diagnostic validity of MRI examinations. Our results correlated with surgical results (reference standard) with perfect interobserver reliability.

Conclusions Of all imaging modalities, MRI has become a prerequisite for a successful surgery of a perianal fistula. MRI can identify: (a) fistula morphological details, (b) the relationship between the fistulous tract and the anal sphincter, (c) fistula wound healing, (d) an active versus chronic scarred fistula, (e) postoperative stigmata, and (f) a perianal fistula from its mimics. MRI with variable sequences and MRI fistulogram are successful combinations that increase diagnostic efficiency with technical safety by avoiding both ionizing radiation and systemic gadolinium.

Keywords Perianal fistula, MRI, MR fistulogram, Diffusion

Background

A perianal fistula is a tract that connects the anal canal or rectum to the skin around the anus. Abscesses and fistulas in the perianal region comprise the same disease process but are at different stages. An abscess is the acute stage, whereas a fistula is a chronic condition [1–3]. Anorectal sepsis and perianal fistulas are common lesions. The incidence rate of perianal fistulas is ~ 1 in 1000 individuals and it usually occurs in adult males with a maximum occurrence in the third to fifth decades [4–7].

*Correspondence:
Asmaa Hagagy Madany
asmaahagagy5@gmail.com
[1] Department of Diagnostic Radiology, Faculty of Medicine, Aswan University, Aswân, Egypt
[2] Department of Diagnostic Radiology, Faculty of Medicine, Assuit University, Asyût, Egypt
[3] Department of General Surgery, Faculty of Medicine, Aswan University, Aswân, Egypt

Fistulas appear as a simple disease; however, both the disease and improper treatment cause significant morbidity [8]. Perianal fistulous disease is divided into two groups: (1) nonspecific and related to anal gland infection, comprising the majority (90%), and (2) related to secondary pelvic pathology, comprising the minority. Cryptoglandular disease is surgically treated by closing the fistula tract and eradicating the infection, whereas other category is medically treated to maintain disease remission [9–12].

The internal sphincter is composed of smooth muscle and, therefore, contracts involuntarily. The external sphincter is composed of striated muscle, and its strong voluntary contractions prevent defecation. Excessive division of the external sphincter leads to fecal incontinence [13]. "Blind" attempts at perianal fistulous tract delineation during surgery lead to unsuccessful treatments. An operation that is too aggressive or too conservative causes disease relapse (infected foci residue) or severe complications such as fecal incontinence (anal sphincter injury) [14].

Successful management of a fistula depends on accurate preoperative anatomical mapping, which is achieved through imaging. Three main imaging techniques are used: contrast fistulography, endoanal ultrasonography, and magnetic resonance imaging (MRI). Each of these methods has advantages and limitations. Selecting the best imaging modality depends on which one provides the most accurate information and application of the "As Low as Reasonably Achievable" (ALARA) principle should be considered in those patients requiring repeated imaging [2, 11–15].

Several studies have discussed the role of MRI in perianal sepsis evaluation [15–18]. Our study is unique because it focused on MRI technical safety. The technique is safely optimized by obtaining an adequate number of sequences, including diffusion and MR fistulogram using water-based contrast media (CM; ultrasonic gel) or gadolinium-based contrast agents (GBCAs) as an alternative (partial substitute) to systemic gadolinium. These patients usually undergo repeated MRI scans; thus, there is a fear of gadolinium deposits in neuronal cells [16]. Our study assessed interobserver agreement for different pulse sequences, including diffusion-weighted images (DWIs) and MR fistulogram.

This study aimed to: (A) evaluate the diagnostic validity of pelvic MRI/MR fistulogram in perianal fistula assessment, (B) elucidate the identification of perianal fistula-associated findings through MRI, and (C) optimize the MRI technique with maximum technical safety by selecting the most appropriate protocol.

Methods

Study design

This prospective diagnostic accuracy multicenter study was conducted at two tertiary care hospitals in Upper Egypt from May 2019 to May 2021.

Ethics approval and consent to participate

The Institutional Review Board approved this study, and informed written consent was obtained from all patients who were included in the study.

Study population

Of 58 cases, 50 were enrolled in the study and 8 were excluded because of the following: (1) narrow or absent external opening ($n=3$); (2) absence of surgical results or medical follow-up ($n=3$); and (3) poor MRI quality due to movement artifacts or the presence of hip implants ($n=2$) (Fig. 1).

Of the patients, 40 (80%) were males and 10 (20%) were females. The age range was between 14 and 75 years, and the mean age ± standard deviation was 42.44 ± 13.29 years.

Inclusion criteria:

- Any age and both genders were eligible
- Patients with a perianal external opening causing discomfort and discharge
- Patients with a history of surgical intervention for a fistula and recurrence
- Patients with renal dysfunction (contraindication to systemic MRI CM) were included because the combination of usual MR sequences with diffusion and MR fistulography could be an adequate alternative to intravenous (IV) CM (especially in simple uncomplicated cases)

Patient assessment

All enrolled patients were subjected to the following:

(1) Detailed clinical examination and history
(2) Laboratory investigations:
    - Renal function tests: serum creatinine and glomerular filtration rate (GFR; $N \geq 60$ mL/min/0.73 m^2).
    - Serum C-reactive protein levels (N < 5 mg/l).
(3) MRI patient preparation included:

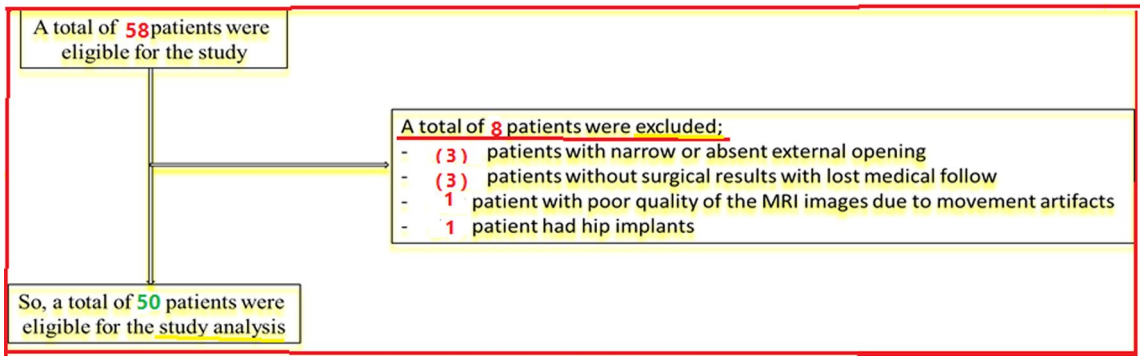

Fig. 1 Number of included and excluded patients

- Removal of all metal objects, such as hearing aids, dentures, jewelry, watches, and hairpins.
- Removal of most clothes and changing into a gown.
- IV line insertion.
- Maintaining a partially full urinary bladder at the time of examination to allow for better pelvic anatomy delineation.
- No special bowel preparation.

Two 1.5 Tesla closed MRI scanners were used for imaging, including a Toshiba Vantage Titan, agent Japan in 34 patients and Siemens Magnetom Sempra, Germany in 16 patients. An external phased-array body coil (covering the region of interest) was used for image acquisition with both machines, and then the patient was iso-centered within the magnet.

MRI examination protocol

- Initial three-plane localizer images were obtained.
- On the sagittal images, the axial cuts were placed parallel to the pelvic diaphragm tilted forward from the vertical by 45° to be perpendicular to the anal canal (oblique).
- Then on the same sagittal plane, the coronal cuts were placed parallel to the anal canal tilted forward from the vertical by 45° to be parallel to the anal canal (oblique).

The acquisition parameters of the applied sequences are displayed in Tables 1 and 2, and various MRI techniques are described. Our study parameters were slightly different according to the machine that was used (Tables 1 and 2).

Table 1 Protocol and applied sequence parameter in 1st institution with 1.5 Tesla system (Toshiba Vantage Titan, agent Japan)

Scan parameters	T2_TSE_sagittal- FS	T2_TSE_axial-FS	T2_TSE_axial oblique	T2_TSE_coronal oblique	T1_TSE_axial oblique_FS	T1_TSE_coronal oblique_FS	DWI
Sequence type	Turbo spin echo (TSE)	Turbo spin echo (TSE)	Turbo spin echo (TSE)	Turbo spin echo (TSE)	Turbo spin echo (TSE)	Turbo spin echo (TSE)	Turbo spin echo (TSE)
Orientation	Sagittal	Axial	Axial oblique	Coronal oblique	Axial oblique	Coronal oblique	Axial oblique
Number of slices	20	30	20	20	26	20	24
Slice thickness (mm)	3.5	3.5	3.6	3	3	3	3
Slice gap (mm)	0.4	0.6	0.6	0.4	0.6	0.6	0.5
FOV (mm)	259 × 360	230 × 320	230 × 320	270 × 320	309 × 380	380 × 380	385 × 385
TR (ms)	4280	6000	6600	6080	730	851	6400
TE (ms)	105	100	134	100	11	15	101
NEX	3	2	2	2	3	3	2
Fat sup	Yes	Yes	No	No	Yes	Yes	-
Matrix	368 × 512	265 × 512	265 × 512	360 × 512	256 × 512	256 × 512	256 × 256
Bandwidth (Hz/Px)	250	250	250	250	195	195	173
B value s/mm^2	–	–	–	–	–	–	0–50–800

Table 2 Protocol and applied sequence parameter in 2nd institution with the 1.5 Tesla system (Magnetom Sempra, Germany)

Scan parameters	T2_TSE_ sagittal_ FS	T2_TSE_axial_ FS	T2_TSE_axial oblique	T2_TSE_coronal oblique	T1_TSE_axial oblique_FS	T1_TSE_coronal oblique_FS	DWI
Sequence type	Turbo spin echo (TSE)	Turbo spin echo (TSE)	Turbo spin echo (TSE)	Turbo spin echo (TSE)	Turbo spin echo (TSE)	Turbo spin echo (TSE)	Turbo spin echo (TSE)
Orientation	Sagittal	Axial	Axial oblique	Coronal oblique	Axial oblique	Coronal oblique	Axial oblique
Number of slices	25	30	25	25	25	20	25
Slice thickness (mm)	3.5	3	3	3	3.5	3.5	3
Slice gap (mm)	0.75	0.6	0.6	0.6	0.75	0.75	0.7
FOV (mm)	320 × 320	220 × 220	220 × 220	254 × 320	210 × 320	210 × 320	250 × 250
TR (ms)	5600	5150	6960	6200	650	650	5800
TE (ms)	95	118	97	117	13	13	80
NEX	3	4	3	2	3	3	2
Fat sup	Yes	Yes	No	No	Yes	Yes	–
Matrix	448 × 336	448 × 336	448 × 336	448 × 336	384 × 216	384 × 216	384 × 216
Bandwidth (Hz/Px)	305	305	305	305	195	195	250
B value s/mm^2	–	–	–	–	–		0–500–1000

Imaging sequences

DW sequences were used to evaluate perianal fistulas, and they were added as routine sequences to provide more accurate evaluations. Following a routine protocol in the supine position (Tables 1 and 2), contrast series were obtained with either intravenous (IV) injection/local (MR fistulogram) or a combined method:

Post-IV contrast T1-weighted imaging (T1WI) with fat saturation was performed in three planes. An injectable solution: Omni scan [Gadodiamide, which is a GBCA, at 287 mg/mL] was used. A bolus IV injection of 0.1 mL/kg (0.05 mmol/kg) was administered, and the IV line was flushed with 5 mL of 0.9% NaCl to ensure complete dosage administration. The imaging procedure was completed within 20 min of administration.

The patient was placed in a prone position for MR fistulography and the site of the fistula opening was cleaned well with alcohol and a povidone-iodine solution. A butterfly cannula without the needle and with the tube cut in a beveled fashion was used for cannulation to facilitate non-traumatic entry. The tip of the cannula was immersed and dipped in xylocaine gel for lubrication and to provide a local anesthetic effect. A total of 1 mL of gadolinium was mixed in 20 mL of sterile normal saline and this solution was gradually injected through the cannula (all air in the syringe was evacuated before the injection). Another solution used in MR fistulography with saline instillation was the ultrasonic gel (T2WI obtained), which facilitated the detection of fistula tracks. The technique, however, depended on the clear existence of a relatively wide external opening at the time of the scan. We closed the opening with sterile gauze and cleaned any contrast refluxed on the skin surface once reflow occurred or there was flow through the second tract and opening.

Both anatomic and active inflammation parameters were evaluated. *Anatomic criteria* (based on the Parks' classification) included: (a) the location of the primary tract, (b) the extension, and (c) the complexity of the tract (single, branched, or multiple). *Inflammatory criteria*, i.e., fistula activity, included: a T2 hyperintense appearance of the fistula tract, presence of hyperintense cavities, and rectal wall thickening. The diagnostic validity of MRI for evaluating perianal fistulas was estimated using surgical findings (mainly), repeated imaging, and clinical follow-up results as reference standards.

Image analysis

Two senior radiologists (A & B) with 15 and 20 years of experience, respectively, in diagnostic radiology independently reviewed the MR images. The obtained study results are presented in a tabulated manner using Microsoft Excel.

Statistical analysis

Data were collected and analyzed using Statistical Package for Social Sciences (SPSS, version 20: IBM Corp., Armonk, New York, USA). The qualitative data were compared using a chi-squared test and Fisher's exact test. The accuracy of MRI with different sequences, including DWI combined with post-contrast series and MR fistulogram in the diagnosis of the perianal fistula and its anatomical characteristics, was statistically analyzed

Table 3 Demographic data of enrolled patients

	***N* = 50**
Age (years)	42.44 ± 13.29
Range	14–75
Age-group	
< 30 years	8 (16%)
31–40 years	19 (38%)
41–50 years	12 (24%)
51–60 years	6 (12%)
> 61 years	5 (10%)
Gender	
Male	40 (80%)
Female	10 (20%)
Pervious fistula operation	6 (12%)
Crohn's disease patients	2 (4%)
Diabetic patients	8 (16%)

Table 4 Parks and St. James classification of perianal fistula in our study

	***N* = 53**
Parks classification	
Intersphincteric	32 (60%)
Trans-sphincteric	13 (24.5%)
Extrasphincteric	4 (7.5%)
Suprasphincteric	4 (7.5%)
St. James classification	
Grade I	23 (43%)
Grade II	10 (19%)
Grade III	8 (15%)
Grade IV	12 (23%)

according to the final surgical results. The degree of agreement between two observers (A and B) regarding CT findings was determined with an interobserver agreement and *K* degrees. The level of confidence was maintained at 95%; hence, *P*-values of < 0.05 were used to denote statistical significance. MRI was reliable in assessing fistulas with very good interobserver concordance ($P < 0.001$). Additionally, sensitivity and specificity with confidence intervals of 95% were defined for the diagnostic procedures.

Results

The most frequent age-group was 31–40 years followed by the 41–50 years age-group. Only five patients were > 61 years old, and six patients had previous fistula operations with recurrence. Two patients presented with Crohn's disease, whereas eight patients had diabetes.

Table 5 Number and site of external opening among enrolled patients

	***N* = 50**
Number of external openings	
Single	46 (92%)
Multiple	4 (8%)
Site of external opening	
6–8 O'clock	35 (70%)
3–5 O'clock	13 (26%)
12–2 O'clock	5 (10%)
9–11 O'clock	2 (4%)

Table 6 Number and site of internal opening among enrolled patients

	***N* = 50**
No. of internal opening	
Single	45 (90%)
Multiple	5 (10%)
Site of internal opening	
6–8 O'clock	27 (54%)
3–5 O'clock	8 (16%)
12–2 O'clock	14 (28%)
9–11 O'clock	6 (12%)

Demographic data of the studied patients are summarized in Table 3.

All patients tolerated the examinations and no side effects were noted. A comprehensive analysis of MRI examinations of 50 patients showed the presence of 50 fistulas (which were correlated with surgical findings and clinical examinations under general anesthesia). The final diagnosis was intersphincteric, trans-sphincteric, extrasphincteric, and suprasphincteric fistulas in 30, 12, 4, and 4 patients, respectively, based on Parks' classification. Based on St. James' classification, 21, 9, 8, 4, and 8 patients were graded as I, II, III, IV, and V, respectively, as given in Table 4.

Of the 50 patients, 46 (92%) had a single *external opening*, whereas 4 (8%) had multiple external openings. In the majority (60%) of patients, the external opening was located at 6–8 o'clock, whereas in 13 (26%), 5 (10%), and 2 (4%) patients, it was located at 3–5, 12–2, and 9–11 o'clock, respectively (Table 5).

Of the 50 patients, 45 (90%) had a single internal opening and 5 (10%) had multiple internal openings. In the majority (44%) of patients, the internal opening was located at 6–8 o'clock, whereas in 8 (16%), 14 (28%), and

Table 7 Validity of MRI and contrast series in diagnosis of different types of perianal fistula

Pathological lesions	Sensitivity (%)	Specificity (%)	PPV	NPV	Accuracy
Perianal fistula	100	100	100	100	100
2ry tract	83	100	100	95	96
Abscess	100	100	100	100	100

NB values are given as percentage: *NPV* Negative predictive value; *PPV* Positive predictive value

Table 8 Presence of secondary tract and abscess among enrolled patients

Associated findings	*N* = 50
Secondary tract	10 (20%)
Horseshoe extension	5 (10%)
Abscess (its presence)	11 (22%)
Site of abscess	
Intersphincteric region	5 (10%)
Ischiorectal fossa	3 (6%)
Around anal canal	2 (4%)
Supralevator region	1 (2%)
Supralevator extension	4 (8%)

Data expressed as frequency (percentage)

Table 9 Degree of agreement between MRI findings and surgery

	Kappa value	95% CI	Degree of agreement
Site of internal opening	0.93	0.88–0.94	Very good
Site of abscess	1	1–1	Almost perfect
St. James classification	0.90	0.80–0.91	Very good
Parks classification	0.91	0.90–0.93	Very good

CI Confidence interval

6 (12%) patients, it was located at 3–5, 12–2, and 9–11 o'clock, respectively (Table 6).

MRI showed 83% sensitivity, 100% specificity, and 96% overall accuracy in detecting the secondary tract and 100% sensitivity, specificity, and overall accuracy in detecting *abscesses* based on correlations with surgical findings (Table 7).

A secondary tract was observed in 10 (20%) patients and an abscess in 11 (22%) patients. Abscesses were located in the intersphincteric region, ischiorectal fossa, around the anal canal, and supralevator region in five (10%), three (6%), two (4%), and one (2%) patients, respectively. Horseshoe and supralevator extensions were found in five (10%) and four (8%) patients, respectively (Table 8).

A local injection was given to 40 patients and, satisfactorily, 38 cases needed no further systemic IV injection. Two cases needed further IV contrast injection, which displayed distended abscess-like loculation, to confirm the diagnosis. Systemic IV CM was injected in 10 patients from the start, and they were clinically diagnosed as having a perianal abscess or complicated recurrence postoperatively.

Surgical treatment was the main line of management in 40 (80%) patients. No surgical procedure was attempted on eight patients because they refused surgery. Another two patients with extrasphincteric-type perianal fistulas and underlying Crohn's disease received medical treatment.

MRI results were in concordance with surgical findings. MRI showed very good agreement with surgeries regarding the site of the internal opening ($K = 0.93$) based on St. James' grading ($K = 0.90$) and Parks' classification ($K = 0.91$) and there was a perfect agreement with the surgery regarding the abscess site ($K = 1$; Table 9).

Follow-up to confirm the imaging diagnosis in each category showed the following:

(1) Intraobserver agreement and interobserver agreement were found for two radiologists (A and B) who independently reviewed all of the data; (2) imaging diagnoses correlated with intraoperative findings (feedback on operated cases through referring doctors); and (3) medically treated cases (inflammatory lesions) were followed up after medical treatment completion.

The two observers (A and B) had very good agreement regarding MRI findings on the secondary tract ($K = 0.89$), site of the internal opening ($K = 0.93$), site of the abscess ($K = 0.98$), St. James' classification ($K = 0.94$), Parks' classification ($K = 0.93$), and overall findings ($K = 0.94$), whereas there was perfect agreement regarding the presence of an abscess ($K = 1$; Table 10).

It was found that DWI had the best diagnostic accuracy (70%) for predictions of abscesses among the studied patients, with an area under the curve (AUC) of 0.808. Although the combination of T2WI and DWI had the same sensitivity (100%), this combination had higher accuracy, reaching 92.3% (Fig. 2) with an AUC of 0.942 (Table 11).

A total of 45 (90%) patients had active tracts and the other five patients had fibrosed inactive tracts. Patients with active tracts had significantly higher apparent diffusion coefficient (ADC) in comparison to those with inactive fibrosed tracts (0.91 ± 0.27 vs. 1.30 ± 0.10 (10^{-3} mm^2/sec); $P < 0.001$). To predict the presence of an active tract, at the cutoff point < 1.1, the ADC had an 86% accuracy (Fig. 3) with an area under the curve of 1 (Table 12).

Discussion

The anatomy of the anal and perianal regions is complex. Perianal sepsis is one of several pathologies that can be identified within this confined anatomical space [18–20]. Successful anal fistula treatment requires a balance between complete eradication of infective foci and maintenance of continence [2, 8, 21–24].

Appropriate MRI standards (various protocols) should be tailored to match the needs of each patient. To the best of our knowledge, our study is unique in limiting the

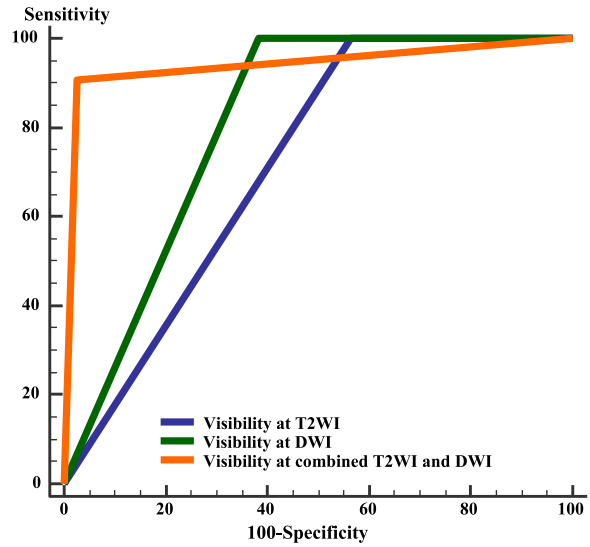

Fig. 2 Accuracy of the MRI technique for predicting abscesses among the studied patients

Table 10 Interobserver agreement between observer A and B for findings in MRI

Findings	Observer A	Observer B	*K* degree	95% CI	*P* value	Percentage (%)
Secondary tract						
Present	8 (16%)	7 (14%)	0.89	0.78–0.9	< 0.0001	92
Absent	42 (84%)	43 (86%)				
Site of internal opening						
6–8 O'clock	27 (54%)	28 (56%)	0.93	0.81–0.98	< 0.001	96
3–5 O'clock	8 (16%)	15 (30%)				
12–2 O'clock	14 (28%)	29 (58%)				
9–11 O'clock	6 (12%)	11 (22%)				
Presence of abscess						
Yes	10 (20%)	10(20%)	1	1	< 0.001	100
No	40 (80%)	40 (80%)				
Site of abscess						
Intersphincteric region	5 (10%)	5 (10%)	0.98	0.91–1	< 0.001	98
Ischiorectal fossa	3 (6%)	3 (6%)				
Around anal canal	2 (4%)	3 (6%)				
Supralevator region	1 (2%)	0				
St. James classification						
Grade I	21(42%)	21 (42%)	0.94	0.89–0.98	< 0.001	96
Grade II	9 (18%)	9 (18%)				
Grade III	8 (16%)	9 (18%)				
Grade IV	12 (24%)	11 (22%)				
Parks classification						
Extrasphincteric	4 (8%)	4 (8%)	0.93	0.81–0.98	< 0.001	96
Intrasphincteric	30 (60%)	29 (58%)				
Suprasphincteric	4 (8%)	5 (10%)				
Trans-sphincteric	12 (24%)	12 (24%)				

P value was significant if < 0.05. *CI* Confidence interval

Interobserver agreement: Interobserver agreement between 2 senior radiologists on the interpretation of images was measured using the kappa statistic, Kappa values: < 0 = no agreement, 0.0–0.20 = slight agreement, 0.21–0.40 = fair agreement, 0.41–0.60 = moderate agreement, 0.61–0.80 = good agreement, and 0.81–1.00 = very good agreement

Table 11 Accuracy of MRI technique in prediction of abscess among studied patients

	Technique		
	T2WI	**DWI**	**Combined T2WI and DWI**
SE	100%	100%	97%
SP	44%	61.5%	91%
PPV	33.3%	42.3%	75%
NPV	100%	100%	99%
AC	56%	70%	92.3%
Cutoff point	> 1	> 1	> 1
AUC	0.718	0.808	0.942
P value	< 0.001	< 0.001	< 0.001

SE Sensitivity, *SP* Specificity; *PPV* Positive predictive value, *NPV* Negative predictive value; *AC* Accuracy; *AUC* Area under the curve

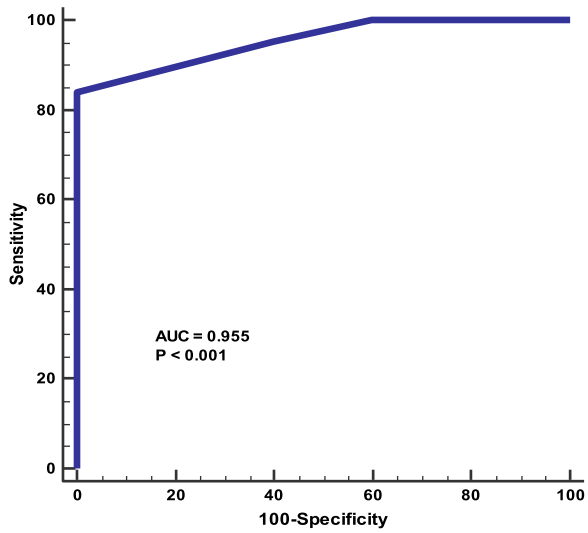

Fig. 3 Accuracy of the apparent diffusion coefficient (ADC) in prediction of active tracts among the studied patients

Table 12 Accuracy of ADC in prediction of active tract among studied patients

Indices	Value
SE	84%
SP	100%
PPV	100%
NPV	41.7%
AC	86%
Cutoff point	< 1.1
AUC	0.955
P value	< 0.001

SE Sensitivity, *SP* Specificity; *PPV* Positive predictive value, *NPV* Negative predictive value; *AC* Accuracy; *AUC* Area under the curve

systemic use of GBCA, with an emphasis on local injection (MRI fistulogram).

Halligan and Stoker [22] and O'Malley [23] concluded that MRI is very sensitive to all types of perianal fistulas. MRI was proven to be superior to other imaging modalities in disease extension assessment with recorded sensitivities and specificities for the fistula and abscesses of > 90%. Our results agreed with previous results as we reported that MRI had 83% sensitivity, 100% specificity, and 96% overall accuracy in detecting the secondary tract and 100% sensitivity, specificity, and overall accuracy in detecting abscesses based on surgical findings.

MRI has a valuable role in determining *grading systems*. The most prevalent type of fistula in the 50 patients in this study was the intersphincteric type followed by the trans-sphincteric type [30 (60%) patients and 12 (24%) patients, respectively]. The suprasphincteric type and extrasphincteric type were found in four (8%) patients each. Our results were consistent with those reported by Liang et al. [24], who revealed the intersphincteric type of fistula was the most reported in their study (70%) followed by trans-sphincteric in 23%, suprasphincteric in 5%, and extrasphincteric in 2% of the patients. Morris et al. [25] recorded a similar pattern with 70% of all perianal fistulas being intersphincteric fistulas, whereas 20% of the total were trans-sphincteric fistulas (Fig. 4).

Baskan et al. [26] revealed that 51.5% had a grade 1 or simple linear intersphincteric fistula, 18.4% had a grade 2 or intersphincteric fistula with an abscess or secondary tract, 11.76% had a grade 3 or trans-sphincteric fistula, 12.3% had a grade 4 or trans-sphincteric fistula with an abscess or secondary track in the ischioanal or the ischiorectal fossa, and 1.5% had grade 5 or supralevator and translevator disease (based on St. James' classification). In our study, 21 (42%), 9 (18%), 8 (16%), 4 (8%), and 8 (16%) patients had perianal fistulas that were grades I, II, III, IV, and V, respectively, based on St. James' classification.

Bayrak et al. [2] revealed that MRI is the modality of choice to assess morphological imaging characteristics. Preoperative MRI imaging should be routine, not only because of its utmost role in determining the relationship of the fistulous tract to the sphincter complex, but also in picking up any *secondary tracts* or *hidden deep foci of infection*. This coincides with our results in which the diagnostic validity of MRI versus surgical findings (reference standard) had 83% sensitivity, 100% specificity, and 96% overall accuracy in detecting the secondary tract. Additionally, it has 100% sensitivity, specificity, and overall accuracy in detecting *abscesses*.

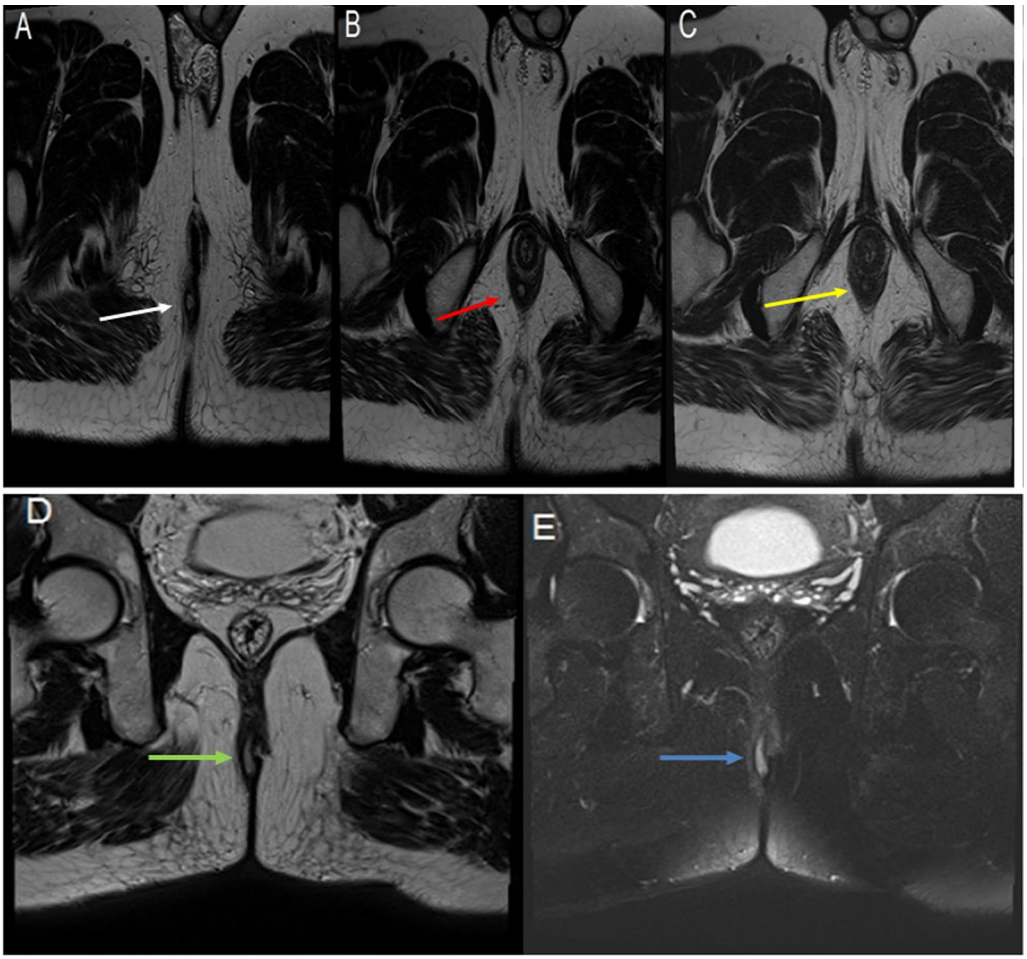

Fig. 4 A 66-year-old male patient who presented with right perianal discharge. MRI examination after local injection of US gel through the fistulous tract revealed through axial T2 images (**A**–**C**): **A** External cutaneous opening of the fistulous tract (white arrow). **B** A non-branching simple tract at the right intersphincteric space (red arrow). **C** Internal mucosal opening connected to the anal canal at six o'clock (yellow arrow). Coronal T2 images showed: **D** the course of the linear intersphincteric tract (green arrow). **E** A coronal STIR image showed hyper-intense signal of the right intersphincteric tract (blue arrow). The final diagnosis was a right, grade I, intersphincteric fistula

Considering the interobserver agreement between the two senior radiologists (interrater reliability), perianal fistula-associated findings were measured using the kappa statistic, which indicated very good agreement.

Regarding the patients' ages, Singh et al. [27] revealed that the mean age for perianal fistulas was 42 years (range, 22–70). In the present study, the mean age of the enrolled patients was 42.44 ± 13.29 years (range, 14–75 years). The most frequent age-group was 31–40 years (38%), followed by 41–50 years (24%). Only five patients were > 61 years old (Fig. 5).

Singh et al. [27] revealed that 45 (90%) patients were males and five (10%) were females. Our study included 40 (80%) males and 10 (20%) females. Mocanu et al. [28] included 817 patients and revealed that one-fifth of the patients with a perianal fistula were females and of a younger age-group (mean age, 30 years).

Sahnan et al. [29] analyzed the data from a wide group of patients with perianal abscess development to perianal fistula formation and revealed that female gender is a risk factor (hazard ratio: 1.18; $P < 0.001$) for fistula formation. Kelley et al. [30] revealed female predominance due to adjacent vaginal problems and the risks associated with childbirth. The present study revealed that perianal fistulas occurred predominantly in adult males with a male-to-female ratio of 4:1 and the mean age of disease was 40 years, which is consistent with previous reports. However, this differed from Singh et al. [27] as they observed a male-to-female ratio of 9:1. These differences might be due to different study populations and dietary or cultural factors.

Vo et al. [31] identified the external opening in 353 of 367 (96.2%) patients with 442 external openings, including 289 (81.9%) patients with one external opening and

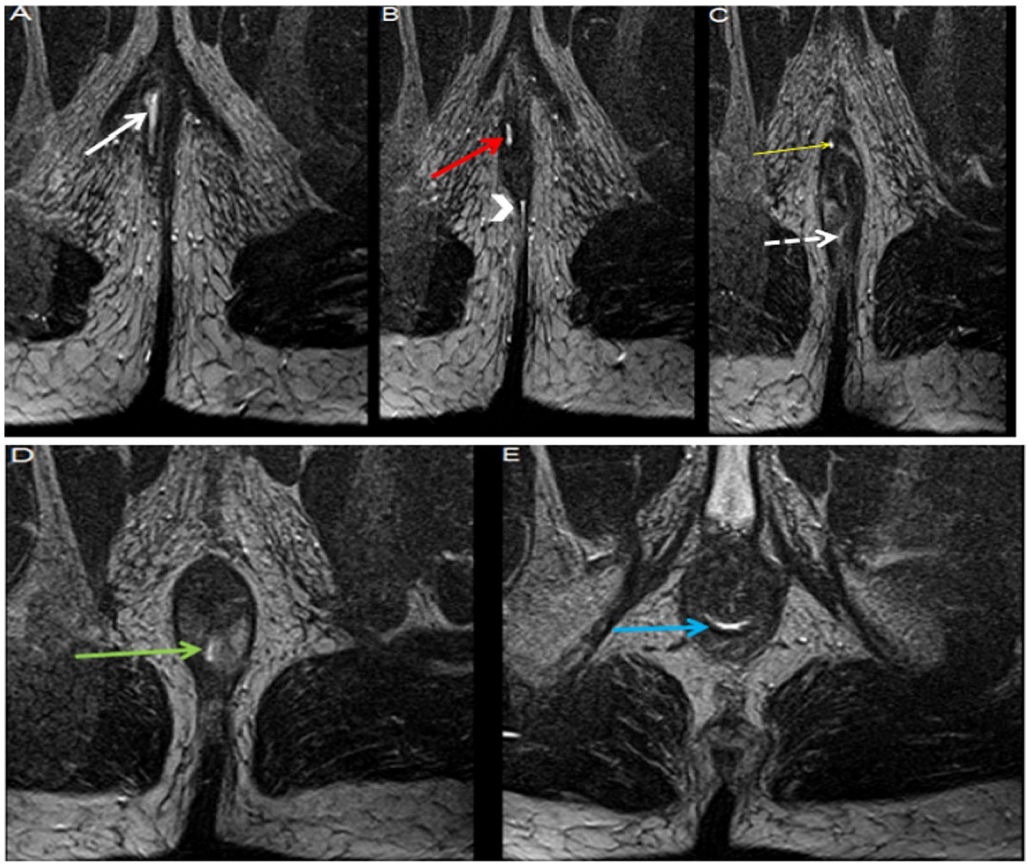

Fig. 5 A 50-year-old male patient presented with discharging fistulous openings. MRI examination in the form of multiple pulse sequences after local injection of saline and gel revealed in axial T2 images (**A**–**E**): **A** External cutaneous opening of the fistulous tract at the right perianal region (white arrow). **B** Fistulous tract at the intersphincteric space (red arrow) with another posterior midline fistulous tract (arrowhead). **C** Internal mucosal opening at 11 o'clock (yellow arrow). The posterior midline tract was seen in the intersphincteric space (dashed arrow). **D** The internal mucosal opening of the posterior midline tract was located in the anal canal at six o'clock (green arrow). **E** Extended branches on both sides of the anal canal giving a horseshoe appearance (blue arrow). The final diagnosis was a right, grade II, intersphincteric fistula

64 (18.1%) patients with multiple external openings, of whom 47 (73.4%) had two, 10 (15.6%) had three, 6 (9.4%) had four, and 1 (1.6%) had five external openings. The external openings in 60.4% were in the posterior perianal skin. Our study revealed that 46 (92%) patients had a single external opening, whereas four (8%) had multiple external openings. In the majority (60%) of patients, the external opening was located at 6–8 o'clock, whereas in 13 (26%), five (10%), and two (4%) patients, it was located at 3–5, 12–2, and 9–11 o'clock, respectively (Fig. 6).

VO et al. [31] determined 385 internal openings (multiple openings can be present in one case) in 367 patients, including 360 (93.5%) internal openings that were located posteriorly at the six o'clock position. The internal opening was recognized in enhanced T1WI, T2WI, and STIR images. Notably, the internal opening location is vital because this will determine the extent of sphincter division during fistulotomy [32]. Our study revealed that 45 (90%) patients had a single internal opening and five (10%) had multiple internal openings. In the majority (44%) of patients, the internal opening was located at 6–8

(See figure on next page.)

Fig. 6 A 58-year-old male patient who complained of left perianal discharge. MRI in the form of multiple pulse sequences revealed in axial T2W images (**A**–**D**): **A** External cutaneous opening of the fistulous tract in the left perianal region (white arrow). **B** Fistulous tract at the left ischioanal fossa (red arrow). **C** The fistulous tract passed through the external sphincter (yellow arrow). **D** Internal mucosal opening at six o'clock (blue arrow). DWI showed (**E**, **F**): hyper-intense signal of the fistulous tract. ADC images (**G**, **H**) showed: a hypo-intense signal of the fistulous tract denoting restriction. The final diagnosis was a left, grade III, trans-sphincteric fistula

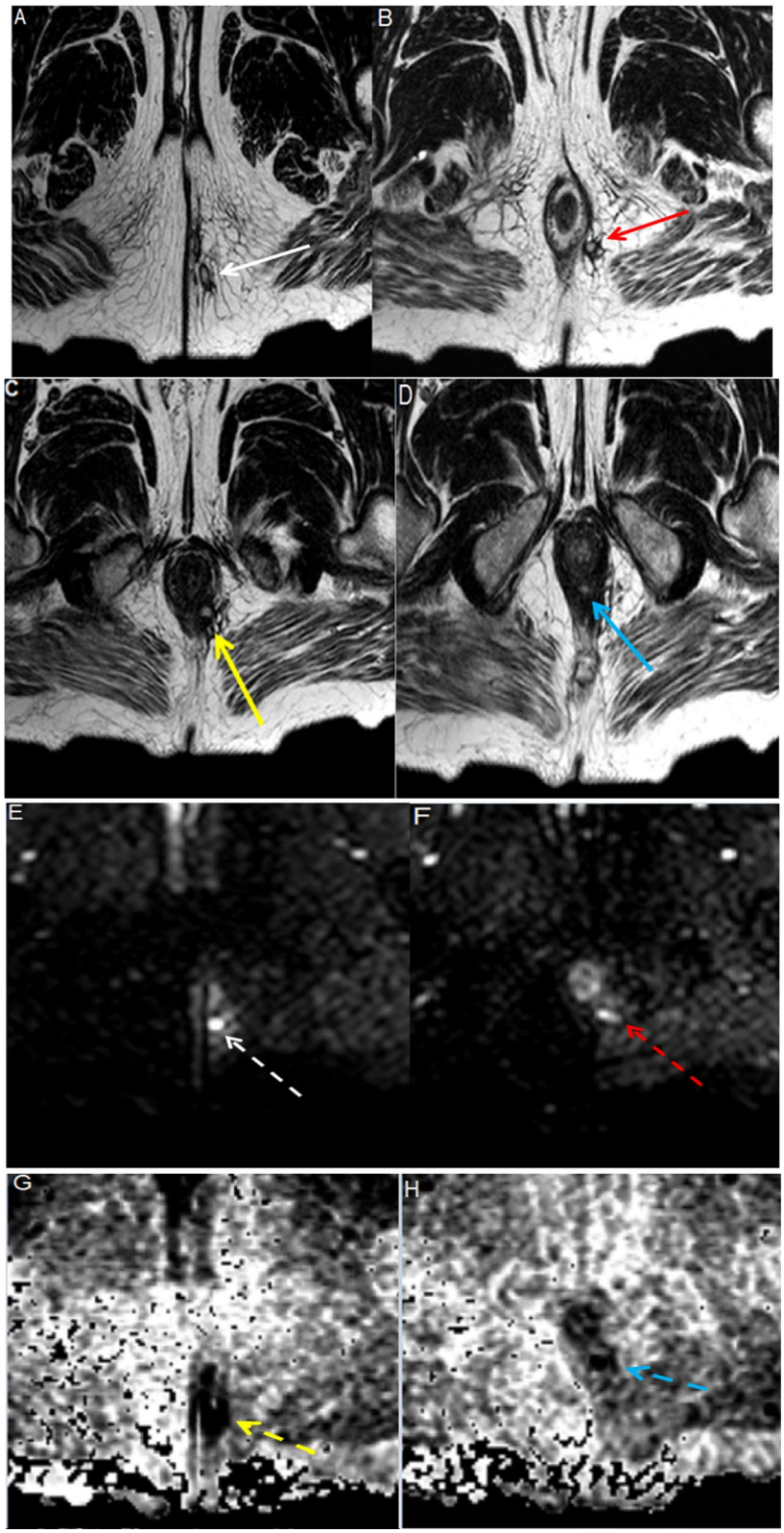

Fig. 6 (See legend on previous page.)

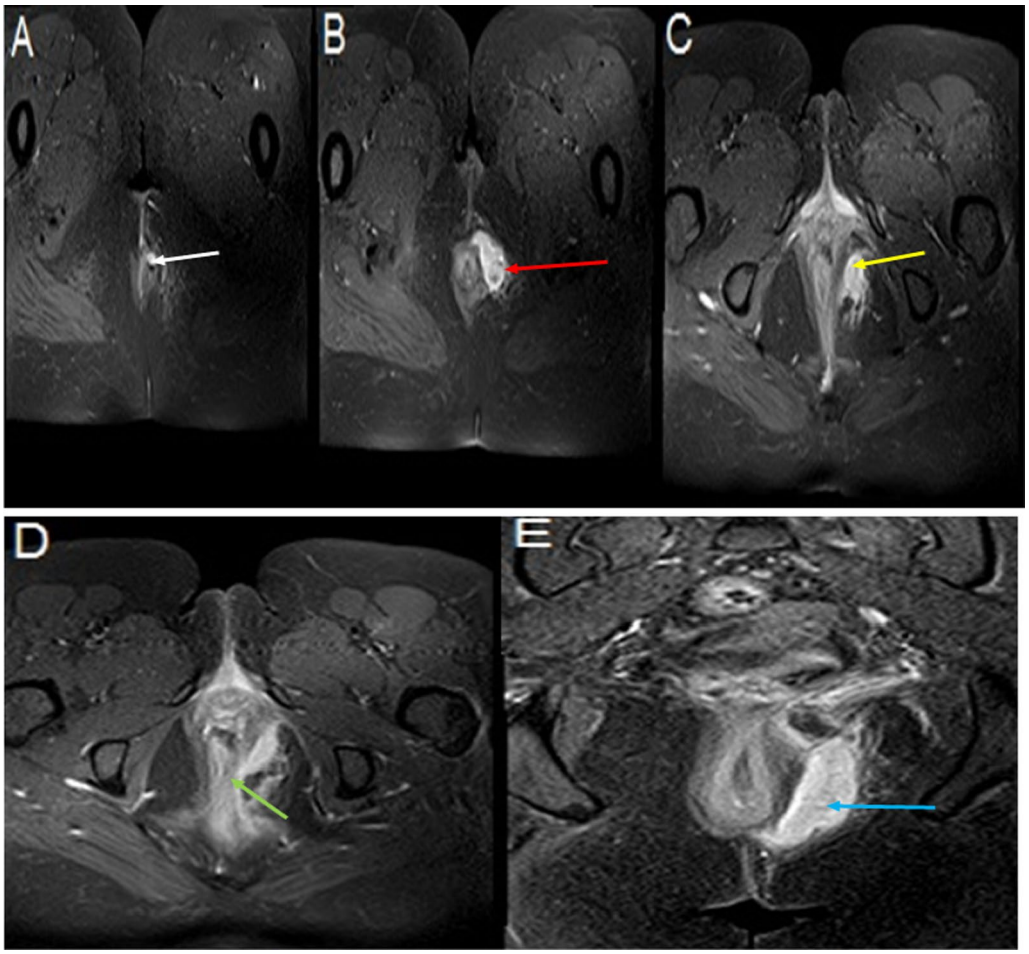

Fig. 7 A 35-year-old female patient presented with left perianal discharge. She was diagnosed clinically with a perianal abscess. Therefore, from the start, we injected IV contrast material. MRI examination after IV contrast injection revealed in enhanced axial T1 FATSAT images (**A**–**D**): **A** External cutaneous opening of the fistulous tract in the left perianal region (white arrow). **B** Distended cavity with peripheral enhancement at the left ischioanal fossa denoting abscess formation (red arrow). **C** An abscess ascending upward and piercing the left levator ani muscle with supralevator extension (yellow arrow). **D** Internal mucosal opening at the anorectal junction at four o'clock (green arrow). **E** Enhanced coronal T1 FATSAT image shows the course of the left extrasphincteric fistula (blue arrow). The final diagnosis was a left, grade V, extrasphincteric fistula

o'clock, whereas in eight (16%), 14 (28%), and six (12%) patients, it was located at 3–5, 12–2, and 9–11 o'clock, respectively.

Patil et al. [33] revealed that MRI is very useful when monitoring the healing of a perianal fistula. The dominant role of contrast-enhanced MRI is the differentiation of active and chronic perianal fistulous tracts. On enhanced MRI, active tracts appear as high signal intensity (S.I.) on fat-suppressed T2W images with intense enhancement on post-contrast images (Fig. 7).

MRI clearly distinguishes anal sphincter, active or inactive lesions, chronic fibrosed fistula, and scarring (through S.I., contrast enhancement and diffusion study). The outer layer of the sphincter complex, the external sphincter, appears hypointense on all pulse sequences. The internal sphincter appears hyperintense on T2WI and enhances the following CM administration. T1WI provides anatomical details of the sphincter complex and the levator plate, whereas T2W and fat-saturated images highlight the tract against pelvic anatomical structures [17, 20, 32–34].

Fistulous tracts show low to intermediate S.I. on T1WI and hyperintense signal on T2W. STIR images with enhancement after contrast injection show active disease and early phases of healing. Chronic fibrosed fistula tracts show a hypointense signal on T1WI and T2WI and did not enhance after CM injection [21, 35].

Loss of hyperintense signal on T2WI followed by an absence of contrast enhancement is a predictable sequence of morphological changes that occur with fistula tract healing [36–38]. This is in agreement with our study in which axial T2W fat-suppressed images were

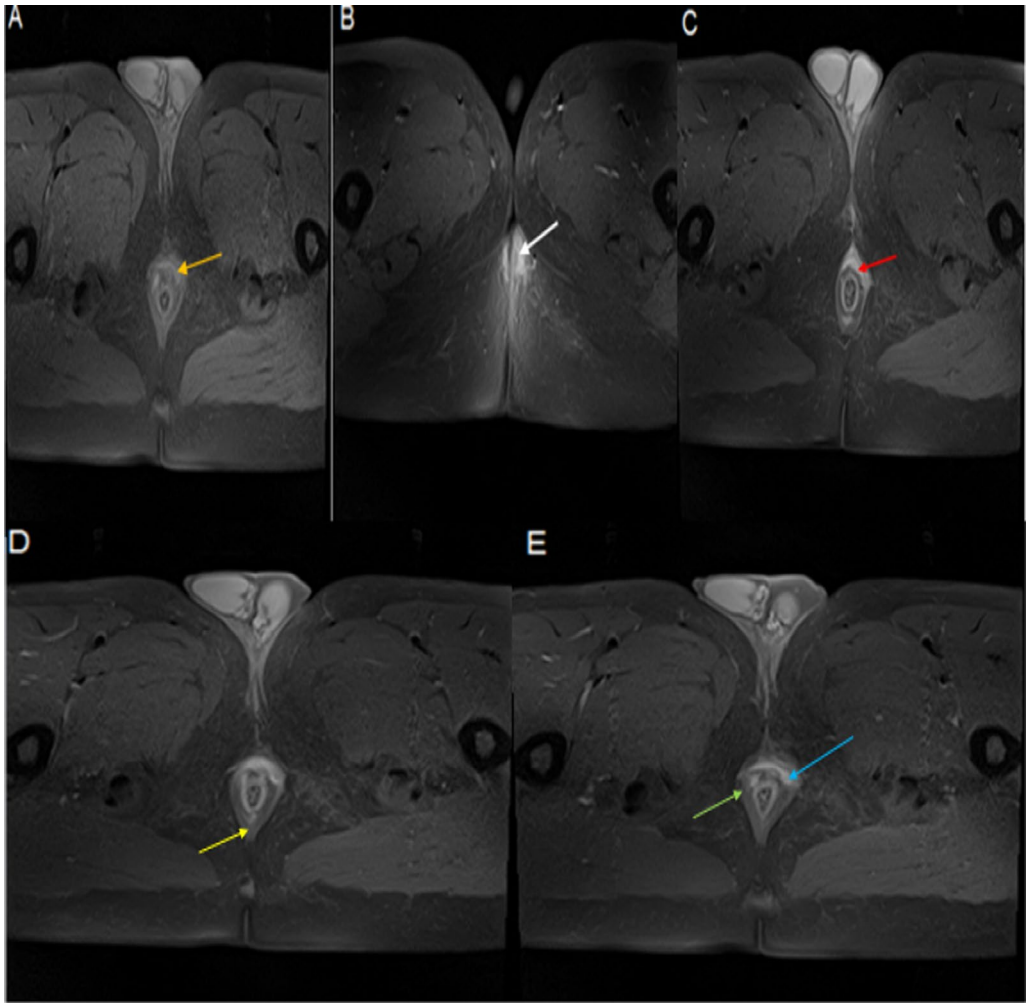

Fig. 8 A 40-year-old diabetic male patient complaining of recurrent perianal fistula after surgery. MRI examination in the form of multiple pulse sequences after IV contrast injection revealed in pre-contrast axial Fat Sat T1 images: **A** a faint horseshoe fistulous tract at the intersphincteric space (orange arrow). Post-contrast axial Fat Sat T1 images (**B**–**E**) showed: **B** external cutaneous opening of the branched fistulous tract in the left perianal region (white arrow). **C** An enhanced fistulous tract seen in the intersphincteric space with secondary branches (red arrow). **D** One branch seen connected with the anal canal at six o'clock (yellow arrow). **E** The enhanced fistulous tract forming a horseshoe extension (blue arrow) connected with the anal canal at 11 o'clock (green arrow). The final diagnosis was a left, grade II, intersphincteric fistula

the most useful sequence for locating a fistulous tract, and after gadolinium injection at T1WI, the tract wall was enhanced, whereas the central portion was hypointense. Abscesses were well depicted in post-gadolinium images. Additionally, our study demonstrated that local contrast injection helps to distend the tract, and IV contrast was better at delineating secondary complications, such as abscesses (Fig. 8).

Mohsen and Osman [39] reported that DWI greatly contributed to this issue. Combined T2WI and DWI was not different (same accuracy) from the combined T2WI and post-contrast images. Our study results were consistent with previous reports as DWI has a vital role in the diagnosis of perianal fistulas and their activity. To predict the presence of an active tract, the cutoff point was < 1.1.

Currently, MRI is used to monitor the effect of medical treatment, e.g., Van Assche MR imaging-based scoring system. Responses in Crohn's disease to biological therapy are observed. Mostly, Crohn's disease-related fistulas have complex features and require medical treatment to induce and maintain disease remission, rather than surgery [40]. The present study reported two patients who were diagnosed with Crohn's disease with complicated fistulas. Responses to medical treatment were recorded such as decreased sepsis and healing of fistulas.

MRI can differentiate perianal fistulas from their mimics. The absence of intersphincteric extension is a key

feature when differentiating various anal and perianal inflammatory conditions, such as hidradenitis suppuravita and pilonidal sinus. In our study, we were confronted with the above-mentioned cases (excluded from the study as the external opening had no discharge or was not connected with the anal canal). Obviously, MRI discriminated between these lesions [41].

MRI can identify postoperative stigmata in patients that are evaluated after fistula surgery; e.g., fat packing (hyperintense on T1WI with suppression in fat-sat sequences), Seton threads (hypointense on T1WI and T2WI), air foci (focal low signal on T1WI and T2WI), and scarring with a disfigured anatomy [42]. Our study revealed seven cases with postoperative features in the form of Seton threads and fat packing, which were easily identified.

Generally, MRI is considered to be safe technology. It can change the position of atoms, but not their structure, composition, and properties, as opposed to ionizing radiation [43]. For the sake of patient safety, the lack of ionizing radiation permits repeated imaging (common status in perianal fistula because hidden infection foci lead to relapse and to monitor treatment effects). Thus, MRI provides the long-term benefit of avoiding ionizing radiation [44].

Another MRI technical issue is the intensive use of GBCA. Nephrogenic systemic fibrosis (NSF) is a known disease process that involves fibrosis of the skin and internal organs, which is observed in some patients with altered or normal renal function. However, individuals with normal renal function can develop gadolinium deposition disease (GDD), and the use of chelating agents is suitable for the treatment of this condition. Improper use of chelation treatment can increase the risk of significant harm from the adverse effects of chelation. Therefore, clinicians should confirm the relevance of gadolinium even in patients with normal renal function [45].

During our study period, there were no contrast media problems at either of the two centers. We limited the use of systemic gadolinium to only complicated cases (two patients, ~ 4%), recurrent, secondary or inquiry cases (10 patients ~ 20%). Imaging in our entire enrolled patient population was well tolerated, with no evidence of contrast medium-related complications (during the study period).

Our present study optimized the MRI technique through the successful combination of MR fistulogram using water-based CM, locally injecting GBCA, and acquiring an adequate number of sequences, including DWI. We use this protocol as an alternative to an enhanced MRI (*to decrease the systemic use of GBCA*) in the majority of our studied patients (38 cases ~ 76%).

Limitations

Most cases in our study were primary and only a few were secondary to Crohn's disease. No cases were associated with anorectal carcinoma or radiotherapy. Moreover, no recurrent or postoperative fistula cases were associated with scar formation and anatomy distortion. This study did not identify the application of diffusion tensor imaging to anorectal sepsis as the technique was not available on our machines.

Future directions

(1) Three-dimensional (3D) T2-weighted turbo spin echo sequences are newer modalities in MRI. This technology can replace multiple 2D T2-weighted sequences. These techniques were used in rectal cancer and the female pelvis, but have not yet been used for fistula imaging. (2) More novel techniques have been developed using post-processing software packages. These input DICOM images can be used to develop 3D perianal fistula models. (3) Combination of the sonographic techniques (EAU and TPUS) may add some benefits if used in the future. 4) Researchers are investigating whether the nature of dynamic enhancement can present prognostic information regarding Crohn's disease [46, 47].

Conclusions

MRI has become a prerequisite for a successful surgical procedure on perianal fistulas due to its sensitivity to all types of perianal fistulas. MRI is highly accurate in identifying fistulous tracts, ramifications, related occult collections, and their relation to the anal sphincter. Additionally, MR adequately monitors the treatment response and discriminates actively against chronic fistula tracts and postoperative stigmata. Moreover, MRI can differentiate a perianal fistula from its mimics.

Variable MR sequences, including diffusion and MR fistulography using water-based contrast agents (e.g., ultrasonic gel) or GBCA (locally), are a successful combination that increases the diagnostic efficiency of MRI examinations and adds MR technical safety by avoiding gadolinium systemic use. This tailored MRI protocol prevents the risk of ionizing radiation, reduces the risk of GDD and NSF conditions, and preserves the use of a systemic GBCA for complicated cases only.

Abbreviations

ALARA	As low as reasonably achievable
CM	Contrast media
CRP	C-reactive protein
DWI	Diffusion-weighted images
EAUS	Endoanal ultrasonography
GBCA	Gadolinium-based contrast agents
GDD	Gadolinium deposition disease

IV	Intravenous
MRI	Magnetic resonance imaging
NSF	Nephrogenic systemic fibrosis
S.I.	Signal intensity
STIR	Short Tau inversion recovery
TPUS	Transperineal ultrasonography
TSE	Turbo spin echo
WI	Weighted images

Acknowledgements
Not applicable.

Author contributions
MAH is the guarantor of the integrity of the entire study. AHM and MAF contributed to the study concepts and design. KMM contributed to the literature research. MAH and AHM contributed to the clinical and experimental studies. MAF and KMM contributed to the data analysis. MAF and AHM contributed to the statistical analysis. MAH and KMM contributed to clinical correlation and follow-up outcome. All authors have read and approved the manuscript.

Funding
No source of funding.

Availability of data and materials
The corresponding author is responsible for sending the used data and materials upon request.

Declarations

Ethics approval and consent to participate
The study was approved by the ethical committee of the Radiology and the General surgery Departments of an academic highly specialized multidisciplinary hospital, and an informed written consent was taken from all patients that were included in the study. The ethics committee's reference number is Ref. No. aswu/391/7/19.

Consent for publication
All authors approved the manuscript. All patients included in this research were legible. They gave written informed consent to publish the data contained within this study.

Competing interests
The authors declare that they have no competing interests.

Received: 2 June 2022 Accepted: 22 January 2023
Published online: 06 March 2023

References

1. Tolan DJ (2016) Magnetic resonance imaging for perianal fistula. Semin Ultrasound CT MR 37(4):313–322
2. Bayrak M, Altintaş Y, Alabaz Ö, Çelîktaş M (2020) Contribution of preoperative magnetic resonance imaging in diagnosis and surgical treatment of anal fistula. Cukurova Med J 45(3):1210–1216
3. Garg P, Kaur B, Yagnik VD, Dawka S, Menon GR (2021) Guidelines on postoperative magnetic resonance imaging in patients operated for cryptoglandular anal fistula: experience from 2404 scans. World J Gastroenterol 27(33):5460–5473
4. Erden A (2018) MRI of anal canal: normal anatomy, imaging protocol, and perianal fistulas: part 1. Abdom Radiol 43(6):1334–1352
5. Boruah DK, Hazarika K, Ahmed H et al (2021) Role of diffusion-weighted imaging in the evaluation of perianal fistulae. Indian J Radiol Imaging 31(01):91–101
6. Adityan R, Immanuel JP (2021) The role of diagnostic medical imaging techniques in the evaluation of perianal fistula: a review. Int J Radiol Imaging Technol 7:084
7. Waniczek D, Adamczyk T, Arendt J, Kluczewska E (2015) Direct MRI fistulography with hydrogen peroxide in patients with recurrent perianal fistulas: a new proposal of extended diagnostics. Med Sci Monit Int Med J Exp Clin Res 21:439
8. Lachance S, Boutros M. Anal sonditions: fistula-in-ano. In: Clinical decision making in colorectal surgery 2020, Springer, Cham, pp 101–109
9. Varghese S, Nunna KC (2018) Patterns of perianal fistula in magnetic resonance imaging and its usefulness in their pre surgical evaluation. J Evolut Med Dent Sci-JEMDS 7(21):2621–2627
10. Jayarajah U, Samarasekera DN (2017) Predictive accuracy of Goodsall's rule for fistula-in-ano. Ceylon Med J 62(2):97–99
11. Sahni VA, Ahmad R, Burling D (2008) Which method is best for imaging of perianal fistula? Abdom Imaging 33(1):26–30
12. Tozer PJ, Burling D, Gupta A, Phillips RK, Hart AL (2011) Review article: medical, surgical and radiological management of perianal Crohn's fistulas. Aliment Pharmacol Ther 33(1):5–22
13. Varsamis N, Kosmidis C, Chatzimavroudis G et al (2022) Perianal fistulas: a review with emphasis on preoperative imaging. Adv Med Sci 67(1):114–122
14. Konan A, Onur MR, Özmen MN (2018) The contribution of preoperative MRI to the surgical management of anal fistulas. Diagn Interv Radiol 24(6):321–327
15. Sharma A, Yadav P, Sahu M et al (2020) Current imaging techniques for evaluation of fistula in ano: a review. Egypt J Radiol Nucl Med 51(1):1–8
16. Fahmy DM, Dawoud MG (2017) Value of diffusion weighted MRI in assessment of simple and complicated perianal fistula. Egypt J Radiol Nucl Med 48(3):553–562
17. Daabis N, El Shafey R, Zakaria Y, Elkhadrawy O (2013) Magnetic resonance imaging evaluation of perianal fistula. Egypt J Radiol Nucl Med 44(4):705–711
18. Beets-Tan RG, Beets GL, van der Hoop AG et al (2001) Preoperative MRI of anal fistula: Does it really help the surgeon? Radiology 218(1):75–84
19. Mohamed RE, Abo-Sheisha DM (2014) Role of MRI in pre-operative assessment of ano-rectal fistula. Egypt J Radiol Nucl Med EJRN 45(1):35–47
20. Stoker J, Rociu E, Wiersma T, Laméris JS (2000) Imaging of anorectal disease. Br J Surg 87(1):10–27
21. Gupta R, Kumar S, Kumar A, Tiwari R, Sinha N (2021) Magnetic resonance imaging of perianal fistulas in clinically symptomatic patients and the correlation among plain, contrast, and post jelly MRI fistulography. J Coloproctol 41(3):265–274
22. Halligan S, Stoker J (2006) Imaging of fistula in ano. Radiology 239(1):18–33
23. O'Malley RB, Al-Hawary MM, Kaza RK et al (2012) Rectal imaging: part 2, Perianal fistula evaluation on pelvic MRI—what the radiologist needs to know. AJR Am J Roentgenol 199(1):W43–W53
24. Liang C, Lu Y, Zhao B et al (2014) Imaging of anal fistulas: comparison of computed tomographic fistulography and magnetic resonance imaging. Korean J Radiol 15(6):712–723
25. Morris J, Spencer JA, Ambrose NS (2000) MR imaging classification of perianal fistulas and its implications for patient management. Radiographics 20(3):623–635
26. Baskan O, Koplay M, Sivri M, Erol C (2014) Our experience with MR imaging of perianal fistulas. Pol J Radiol 79:490–497
27. Singh K, Singh N, Thukral CL, Singh KP, Bhalla V (2014) Magnetic resonance imaging (MRI) evaluation of perianal fistulae with surgical correlation. J Clin Diagn Res 8(6):1–4
28. Mocanu V, Dang JT, Ladak F et al (2019) Antibiotic use in prevention of anal fistulas following incision and drainage of anorectal abscesses: a systematic review and meta-analysis. Am J Surg 217(5):910–917
29. Sahnan K, Askari A, Adegbola SO et al (2017) Natural history of anorectal sepsis. Br J Surg 104(13):1857–1865
30. Kelley KA, Kaur T, Tsikitis VL (2017) Perianal Crohn's disease: challenges and solutions. Clin Exp Gastroenterol 10:39–46
31. Vo D, Phan C, Nguyen L et al (2019) The role of magnetic resonance imaging in the preoperative evaluation of anal fistulas. Sci Rep 9(1):1–8
32. Sneider EB, Maykel JA (2013) Anal abscess and fistula. Gastroenterol Clin N Am 42(4):773–784
33. Patil S, Patil S, Nimbal V (2018) Usefulness Assessment of preoperative MRI fistulography in perianal fistulas patients. Int J Contemp Med Surg Radiol 3(3):C21–C24
34. Halligan S (2020) Magnetic resonance imaging of fistula-in-ano. Magn Reson Imaging Clin N Am 28(1):141–151

35. Jabeen N, Qureshi R, Sattar A, Baloch M (2019) Diagnostic accuracy of short tau inversion recovery as a limited protocol for diagnosing perianal fistula. Cureus 11(12):e6398
36. Villa C, Pompili G, Franceschelli G et al (2011) Role of magnetic resonance imaging in evaluation of the activity of perianal Crohn's disease. Eur J Radiol 81(4):616–622
37. Thipphavong S, Costa AF, Ali HA et al (2019) Structured reporting of MRI for perianal fistula. Abdom Radiol 44(4):1295–1305
38. Cavusoglu M, Duran S, Cılız DS et al (2017) Added value of diffusion-weighted magnetic resonance imaging for the diagnosis of perianal fistula. Diagn Interv Imaging 98(5):401–408
39. Mohsen LA, Osman NM (2020) Diffusion-weighted imaging in the evaluation of perianal fistula and abscess. Egypt J Radiol Nucl Med 51(1):1–9
40. Balcı S, Onur MR, Karaosmanoğlu AD et al (2019) MRI evaluation of anal and perianal diseases. Diagn Interv Radiol 25(1):21–27
41. Khera PS, Badawi HA, Afifi AH (2010) MRI in perianal fistulae. Indian J Radiol Imaging 20(1):53–57
42. Puca P, Lopetuso LR, Laterza L, Pizzoferrato M, Scaldaferri F (2022) Clinical assessment of Crohn perianal abscesses and fistulas. In: Anal fistula and abscess, Springer International Publishing, Cham, pp 113–126
43. Gallego JC, Echarri A (2018) Role of magnetic resonance imaging in the management of perianal Crohn's disease. Insights Imaging 9(1):47–58
44. Torkzad MR, Ahlström H, Karlbom U (2014) Comparison of different magnetic resonance imaging sequences for assessment of fistula-in-ano. World J Radiol 6(5):203–209
45. Navkar NV, Balakrishnan S, Kharbech S et al (2022) 3D visualization of perianal fistulas using parametric models. Tech Coloproctol 26(4):291–300
46. ElSharbatly R, Halim M, Shaker F, Mashhour AN, Azzam H (2022) Role of MRI special diffusion weighted imaging/diffusion tensor imaging techniques in the assessment of perianal fistula activity. Egypt J Radiol Nucl Med 53(1):1–9
47. Cerit MN, Öner AY, Yıldız A et al (2020) Perianal fistula mapping at 3 T: volumetric versus conventional MRI sequences. Clin Radiol 75(7):563-e1

Publisher's Note